Group I lytic polysaccharide monooxygenase (LPMO1) is required for efficient chitinous cuticle turnover during insect molting

mingbo Qu
Myeongjin Kim
Xiaoxi Guo
Seulgi Mun
Shuang Tian
Mi Young Noh
Karl J Kramer
Subbaratnam Muthukrishnan
Yasuyuki Arakane
Qing Yang (qingyang@dlut.edu.cn)
Institute of Plant Protection, Chinese Academy of Agricultural Sciences,

Article

Keywords: chitin, chitinolytic enzyme, lytic polysaccharide monooxygenase (LPMO), cuticle, molting

Posted Date: September 13th, 2021

DOI: https://doi.org/10.21203/rs.3.rs-877720/v1

Version of Record: A version of this preprint was published at Communications Biology on May 31st, 2022. See the published version at https://doi.org/10.1038/s42003-022-03469-8.

Group I lytic polysaccharide monooxygenase (LPMO1) is required for efficient chitinous cuticle turnover during insect molting

Mingbo Qu[1†], Myeongjin Kim[4†], Xiaoxi Guo[1], Seulgi Mun[4], Shuang Tian[1], Mi Young Noh[5], Karl J. Kramer[6], Subbaratnam Muthukrishnan[6] and Yasuyuki Arakane[4*], Qing Yang[2, 3*]

[1] School of Bioengineering, Dalian University of Technology, Dalian 116024, China

[2] State Key Laboratory for Biology of Plant Diseases and Insect Pests, Institute of Plant Protection, Chinese Academy of Agricultural Sciences, Beijing 100193, China

[3] Shenzhen Branch, Guangdong Laboratory of Lingnan Modern Agriculture, Genome Analysis Laboratory of the Ministry of Agriculture and Rural Affairs, Agricultural Genomics Institute at Shenzhen, Chinese Academy of Agricultural Sciences, Shenzhen 518120, China

[4]Department of Applied Biology, Chonnam National University, Gwangju 61186, South Korea

[5]Department of Forest Resources, AgriBio Institute of Climate Change Management, Chonnam National University, Gwangju 61186, South Korea

[6]Department of Biochemistry and Molecular Biophysics, Kansas State University, Manhattan, Kansas 66506, USA

[†]Both authors contributed equally to this work.

[*]To whom correspondence may be addressed. Email to QY at qingyang@dlut.edu.cn or to YA at arakane@chonnam.ac.kr.

Abstract

Microbial lytic polysaccharide monooxygenases (LPMOs) catalyze the oxidative cleavage of crystalline polysaccharides including chitin and cellulose. The discovery of a large assortment of LPMO-like proteins widely distributed in insect genomes suggests that they could be involved in assisting chitin degradation in the exoskeleton, tracheae and peritrophic matrix during development. However, the physiological functions of insect LPMO-like proteins are still undetermined. To investigate the functions of insect LPMO subgroup I-like proteins, which contain an AA15 LPMO catalytic domain and a conserved C-terminal cysteine-rich motif, two evolutionarily distant species, *Tribolium castaneum* and *Locusta migratoria*, were chosen for study. RNAi for the *T. castaneum* protein, *TcLPMO1,* caused molting arrest at all developmental stages, whereas RNAi of the *L. migratoria* protein, *LmLPMO1,* prevented only adult eclosion. In both species, LPMO1-deficient animals were unable to shed their exuviae and died. TEM analysis revealed failure of turnover of chitinous cuticle, which is critical for completion of molting. Purified recombinant LPMO1-like protein from *Ostrinia furnacalis* (rOfLPMO1) exhibited oxidative cleavage activity and substrate preference for chitin. These results reveal for the first time the physiological importance of catalytically active LPMO1-like proteins from distant insect species and provide new insight into the enzymatic mechanism of chitin turnover during molting.

Keywords: chitin, chitinolytic enzyme, lytic polysaccharide monooxygenase (LPMO), cuticle, molting

Introduction

Insect cuticle consists of morphologically distinct tissue layers including the outermost envelope, epicuticle and innermost procuticle (exocuticle and endocuticle), the latter consisting of a large number of horizontally oriented chitin-protein rich laminae [1-3]. To accommodate growth, insects periodically replace their cuticle in a process involving ecdysis and molting. The turnover of chitin in the cuticle by enzymes presents several challenges because of the crystallinity of the anti-parallel chitin chains and potential covalent cross-linking to cuticular proteins. The roles of chitinolytic enzymes are relatively well understood [4-6]. However, the functions of lytic polysaccharide monooxygenases (LPMOs) that have the potential to digest insect chitin are less well studied and thus, is the focus of this research.

LPMOs belong to a class of proteins that assist in the degradation of crystalline polymeric carbohydrate substrates (EC 1.14.99.53/54/55/56; https://www.qmul.ac.uk/sbcs/iubmb/enzyme/EC1/1499.html). They are copper-dependent enzymes that catalyze oxidative cleavage of glycosidic bonds in polysaccharides such as chitin, cellulose and starch in the presence of a reductant and oxygen [7]. LPMOs have been identified in a wide range of organisms including bacteria, fungi, viruses, archaea and algae, as well as in higher animals such as cnidaria, mollusks and arthropods [7-10]. They are classified in the Carbohydrate-Active EnZYmes database (CAZy) into eight auxiliary activity (AA) families including AA9 (formerly glycosyl hydrolase family 61, GH61), AA10 (formerly carbohydrate-binding module family 33, CBM33), AA11 and AA13-AA17 enzymes

[8,11-18]. In insects the gene family encoding LPMO-like proteins has been identified recently and determined to belong to the AA15 family. In addition, insect LPMOs of this family could be further classified into several subgroups based on phylogenetic analysis and the presence of additional motifs (see Fig. 1a).

Bacterial LPMOs initially were identified as non-catalytic carbohydrate-binding proteins (CBP21 and CBM33), which enhanced polysaccharide degradation catalyzed by glycosyl hydrolases [19]. However, Vaaje-Kolstad et al. [20] demonstrated subsequently that the proteins CBP21 and CBM33A from *Serratia marcescens* and *Enterococcus faecalis*, respectively, are able to cleave glycosidic bonds of crystalline chitin in an oxidative fashion, creating new access points to the substrate for chitinolytic enzymes. After these initial findings, other enzymatic properties such as substrate specificity and modes of action of LPMOs from microorganisms and viruses were examined extensively. Those studies demonstrated that LPMOs could cleave recalcitrant polysaccharides including chitin, cellulose, starch, xylan, pectin and various other hemicelluloses as well as soluble cello-oligosaccharides [13-15,21-27]. Only a few studies on the enzymatic properties of LPMO-like proteins from insects have been reported so far. For example, Sabbadin et al. [8] identified 23 genes encoding LPMO-like proteins (TdLPMOs) in the transcriptome of the firebrat, *Thermobia domestica* (*Td*), which is an ancient insect species capable of digesting crystalline cellulose by using its own enzymes without the assistance of enzymes from microbial symbionts, with 21 of them (including TdAA15A and TdAA15B) present in the gut proteome. The recombinantly expressed TdAA15A protein, which is one of the most abundant

LPMO-like proteins from *T. domestica*, exhibited synergistic activity with enzymes of glycosylhydrolase families GH6 (cellobiohydrolase) and GH18 (endochitinase) on the breakdown of cellulose and chitin, respectively. In contrast, another recombinant enzyme, TdAA15B, showed activity on crystalline chitin but not on cellulose. Similarly, two recombinant LPMOs (CgAA15a and CgAA15b) from the lower termite, *Coptotermes gestroi*, catalyzed the oxidative cleavage of chitin, but not cellulose, xylan, xyloglucan or starch [28].

The primary role of bacterial LPMOs appears to be the degradation of polysaccharides as a nutrient carbon source. In addition, some studies of entomopathogenic bacteria, oomycetous fungi and viruses have demonstrated their functional importance in pathogenicity. For instance, *Paneibacillus larvae* is a bacterial pathogen that causes a serious disease of honeybees, American Foulbrood (AFB). PlCBP49 protein containing an LPMO domain (AA10 family) of *P. larvae* is critical for the degradation of the chitin-rich peritrophic matrix (PM) in the lining of the midgut of bee larvae, which is a vital step in the invasion of *P. larvae* during infection [29]. *Phytophthora infestans* is a damaging crop pathogenic oomycete that infects both potato and tomato crops. A new family of AA17 LPMO from *P. infestans* has been reported to oxidatively cleave the backbone of pectin, playing an important role as virulence factors [18]. Similarly, spindles produced by entomopoxviruses (EVs) are cellular crystals of the LPMO-domain-containing protein, fusolin (AA10 family). This protein disrupts the host's PM, leading to the greatly enhanced infectivity of EVs [30].

111 Because chitin is a major structural component of insect cuticle, tracheae and the
112 PM [6], LPMO-like proteins could be involved in the degradation of chitin in those
113 tissues during development. However, the exact physiological functions of insect
114 *LPMO* genes are still not determined. In this study, we report on the physiological
115 function of LPMO-like proteins comprising one of the subgroups of insect LPMO
116 (denoted as group I LPMO) whose members have an AA15 LPMO catalytic domain
117 and a conserved long C-terminal stretch of ~120 amino acids containing a
118 cysteine-rich motif. Three economically important agricultural pests from three orders
119 of insects were used as model species to investigate the function of insect LPMO1s.
120 The holometabolous red flour beetle, *Tribolium castaneum* (Coleoptera), and
121 hemimetabolous migratory locust, *Locusta migratoria* (Orthoptera), were utilized to
122 study the biological function(s) of LPMO1s by RNA interference (RNAi), while an
123 LPMO1 from the holometabolous Asian corn borer, *Ostrinia furnacalis* (Lepidoptera),
124 was used to study the enzymatic properties of this class of enzymes. We provide
125 experimental evidence for a functional importance of insect LPMO1s in the catabolic
126 oxidative breakdown of cuticular chitin, which is also degraded by a mixture of
127 molting fluid chitinases and β-*N*-acetylhexosaminidases [4-6]. This work provides new
128 insight into the molecular mechanism underlying the vital process of chitin
129 degradation in insect molting.

Results

Phylogenetic analysis of insect LPMOs

A gene family encoding LPMO-like proteins was found recently in an ancient insect species, *T. domestica*, and several other species including *D. melanogaster* and *C. gestroi* [8,31]. This family is classified as members of auxiliary activity family 15 (AA15) in the Carbohydrate Active enZymes (CAZy) database [17]. By our initial search using the TdAA15A of *T. domestica* as a query, we identified nine genes in the genome of *T. castaneum* that encode LPMO (AA15 family)-like proteins. Using these predicted LPMO protein sequences as queries, we searched other insect genomes that have been fully sequenced and annotated. A phylogenetic analysis of these sequences indicated that insect LPMO-like proteins can be divided into at least four major clusters, which we denoted as groups I (LPMO1s), II (LPMO2s), III (LPMO3s) and IV (lepidopteran-specific LPMOs) (Fig. 1a). Interestingly, 21 TdLPMOs identified in the gut proteome of *T. domestica* [8] comprise a separate clade. The groups *LPMO1* and *LPMO2* present in all orders of *Insecta* appear to have a single representative in all of the species identified, whereas the number of representatives in the *LPMO3* group ranged from one to seven in different species. Note that group III *LPMOs* do not include any representatives from lepidopteran species characterized so far. Instead, there is a separate group with representatives from lepidopterans only, often with more than one member. All LPMO-like proteins identified consist of a putative signal peptide and an AA15 catalytic domain. In addition, LPMO1s have a C-terminal stretch

containing a cysteine-rich motif, whereas LPMO2s from group 2 have a predicted transmembrane span.

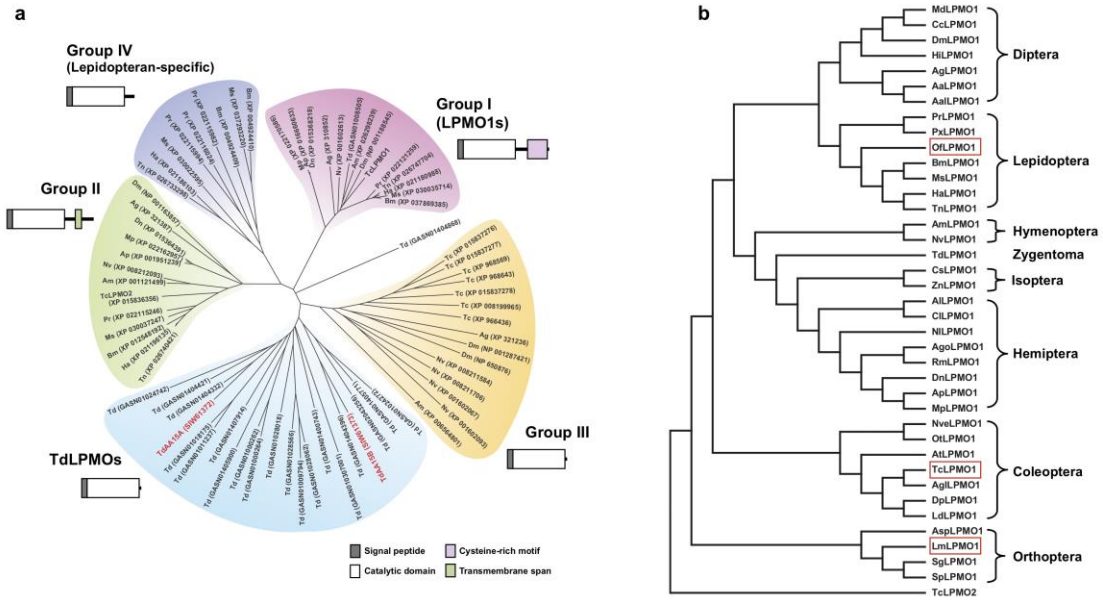

Fig. 1 Phylogenetic analysis of insect LPMOs. a A phylogenetic tree of putative LPMOs from *T. castaneum* and other insects whose genomes have been sequenced and annotated. Tc, *Tribolium castaneum*; Dm, *Drosophila melanogaster*; Ag, *Anopheles gambiae*; Am, *Apis mellifera*; Nv, *Nasonia vitripennis*; Bm, *Bombyx mori*; Ms, *Manduca sexta*; Ha, *Helicoverpa armigera*; Tn, *Trichoplusia ni*; Pr, *Pieris rapae*; AP, *Acyrthosiphon pisum*; Mp, *Myzus persicae*; Dn, *Diuraphis noxia*; Td, *Thermobia domestica*. TdAA15A and TdAA15B are highlighted in red. **b** Phylogenetic tree of insect group I LPMOs (LPMO1s). Amino acid sequences of LPMO1 proteins from different insect species were obtained by performing a BLASTP search of NCBI database. TcLPMO2 (group II LPMO) of *T. castaneum* was used as the outgroup. Phylogenetic trees were constructed by MEGA 7.0 software using the Neighbor-Joining method. See Supplementary Table 2 for the accession numbers of LPMO1 proteins used in this study.

Sequencing of *TcLPMO1*, *LmLPMO1* and *OfLPMO1* cDNAs

For this study we focused only on members of the LPMO1 subgroup because their single-copy orthologous genes encoding not only a AA15 catalytic domain but also a C-terminal cysteine-rich motif are present in all insect orders so far examined, indicating that they are likely to have essential physiological functions. In addition to the insect genomes that have been fully sequenced and annotated, we also performed BLAST searches of the *L. migratoria* and *O. furnacalis* transcriptomes using the TcLPMO1 and/or TdAA15A protein as queries. We identified LPMO1 orthologs from *L. migratoria* (LmLPMO1) and *O. furnacalis* (OfLPMO1) as well as from other species of other insect orders including the Coleoptera, Hymenoptera, Diptera, Hemiptera, Orthoptera and Isoptera (Fig. 1b). Our searches confirmed that there is single member of the LPMO1 subgroup in species of those insect orders and that TcLPMO2 members form an outgroup. The LPMO1 subgroup is of an ancient origin and must have diverged from a common progenitor of the LPMO2 subgroup. Using primers flanking the predicted start and stop codon regions, we were able to amplify *TcLPMO1*, *LmLPMO1* and *OfLPMO1* cDNAs including the entire open reading frames that encode proteins with 337, 339 and 343 amino acid residues and theoretical molecular masses for the mature proteins of 35.8, 34.6 and 35.3 kDa, respectively (Supplementary Fig. 1). Each protein, as seen in the members of group I LPMOs, has a putative signal peptide and a conserved 192 or 193 amino acids-long AA15 catalytic domain followed by a ~120 amino acids-long C-terminal stretch containing a 74 amino acids-cysteine-rich motif that contains two 6-cysteine-containing internal repeats

(C-X_{15}-C-X_3-C-$X_{6\text{-}9}$-C-X_4-C-X_1-C) (*Supplementary* Fig. 2). Sabbadin et al. [8] reported about several amino acid residues that are critical for LPMO activity as revealed by the crystal structure of TdAA15A in the 190 amino acids-long AA15 catalytic domain (see Supplementary Fig. 2); they include two histidines (His1 and His91), which directly coordinate a copper ion with a T-shaped geometry in the catalytic site, known as the histidine brace; alanine (Ala89) and tyrosine (Tyr184), which are also involved in forming the copper-containing active center as non-coordinating amino acid residues occupying the apical site and axial position of the copper ion, respectively; and two other tyrosines (Tyr24 and Tyr166) located at the boundaries of the flat surface surrounding the active center, which could be involved in substrate binding. All insect LPMO1-like proteins in our analysis (Supplementary Fig. 2) have the 192 amino acids-long AA15 catalytic domain except for some orthopteran LPMO1s, which are composed of 193 amino acids. All members of this group share a high degree of amino acid sequence identity/similarity (54-99 and 78-100%, respectively). The catalytically critical amino acid residues (H1, Y24, A/S89, H91, W168/169 and F186/187) occupy the same positions in the sequence alignment. All of them differ from the TdAA15A enzyme in the replacement of Y166 by W168 in the boundaries of the flat surface surrounding the active center and Y184 by F186 in the axial position of the copper-binding site (Supplementary Fig. 2).

Developmental and tissue-specific expression of *LPMO1* genes in *T. castaneum* and *L. migratoria*

To determine the role(s) of LPMO1s in insect development, the expression profiles of *TcLPMO1* and *LmLPMO1* during various growth stages were conducted using real-time PCR. With *T. castaneum*, transcripts of *TcLPMO1* were detected in all developmental stages analyzed with lowest expression in embryos and mature adults and highest expression in the pharate pupal stage (Fig. 2a). During late stages of development from pharate pupae to day 7 adults, high transcript levels of *TcLPMO1* were detected at early pharate pupal (PP1) and early pupal (P0-P2) stages and declined thereafter (Fig. 2b). To assess the tissue specificity of expression of *TcLPMO1*, we dissected late stage larvae to obtain midgut and carcass (whole body minus midgut) tissue preparations. The transcript level of *TcLPMO1* in the carcass was substantially higher than that in the midgut (Fig. 2c).

In *L. migratoria*, the temporal expression pattern of *LmLPMO1* was analyzed during the later stages of development from the 4^{th} instar nymph to the adult stage. Transcripts of *LmLPMO1* were observed at all stages with higher levels detected in the 4^{th} instar day 5 and 5^{th} instar days 1-3 during the nymph-nymph molt (Fig. 2d). The tissue-specific expression analysis showed that *LmLPMO1* is expressed at a higher level in the epidermis than in other tissues analyzed such as the midgut, testis and ovary (Fig. 2e). These results suggest a role of both TcLPMO1 and LmLPMO1 in the turnover of chitin in the cuticle.

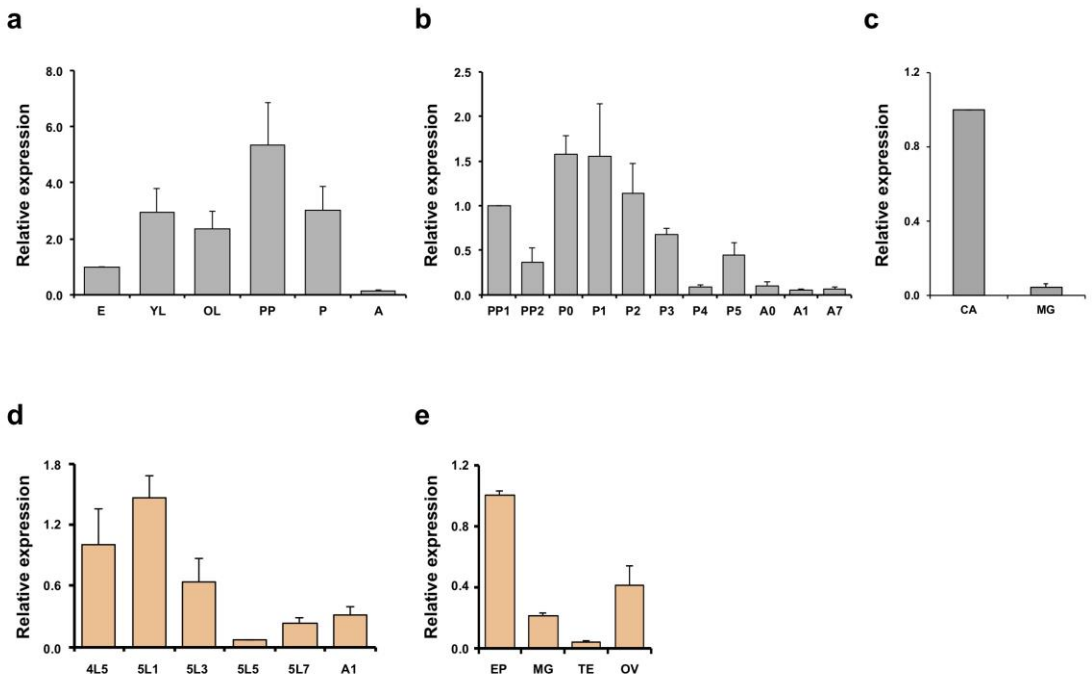

230

231 **Fig. 2 Expression profiles of *TcLPMO1* and *LmLPMO1*. a** Transcript levels of

232 *TcLPMO1* relative to that of *TcRpS6* at the indicated developmental stages of *T.*

233 *castaneum* were determined by real-time PCR. E, embryos; YL, young larvae; OL, old

234 larvae; PP, pharate pupae; P, pupae; A, mature adults. **b** To analyze the expression

235 patterns of *TcLPMO1* at later stages of development, the time points analyzed were

236 expanded between the early pharate pupa to young adult stage. PP1, day 0-1 pharate

237 pupae; PP2, day 1-2 pharate pupae; P0, day 0 pupae; P1, day 1 pupae; P2, day 2 pupae;

238 P3, day 3 pupae; P4, day 4 pupae; P5, day 5 pupae; A0, day 0 adults; A1, day 1 adults;

239 A7, day 7 adults. **c** To analyze the transcript levels of *TcLPMO1* in the carcass (CA,

240 whole body minus midgut) and midgut (MG), cDNA was prepared from total RNA

241 extracted from a pool of tissues of ten actively feeding larvae. **d** Transcript levels of

242 *LmLPMO1* relative to that of *LmRP49* in the epidermis collected from the indicated

243 developmental stages of *L. migratoria* were determined by real-time PCR. 4L5, 4th

244 instar day 5; 5L1, 5th instar day 1; 5L3, 5th instar day 3; 5L5, 5th instar day 5; 5L7, 5th

245 instar day 7; A1, adult day 1. **e** To analyze spatial expression patterns of *LmLPMO1*,
246 total RNA was extracted from the epidermis (EP), midgut (MG), testis (TE) and ovary
247 (OV) from three 5^{th} instar day 3 nymphs. All data are shown as the mean value ± SE (n
248 = 3).
249
250 **Biochemical properties of OfLPMO1**
251 To further illustrate that the LPMO1s participate in the degradation of chitin during
252 molting, we attempted to express the full-length proteins, TcLPMO1s, LmLPMO1 and
253 OfLPMO1 from *T. castaneum*, *L. migratoria* and *O. furnacalis*, respectively, in yeast
254 cells. Only the recombinant expression of OfLPMO1, which shares an amino acid
255 sequence identity of 71% and 63% with those of TcLPMO1 and LmLPMO1,
256 respectively, was successful (Fig. 3a). The recombinant OfLPMO1 was found to have a
257 peroxidase activity when using 2,6-dimethoxyphenol (2,6-DMP) as a chromogenic
258 substrate and H_2O_2 as a co-substrate at pH 6.0 and 30°C (Fig. 3b). The reaction was
259 linear over a 10-minute reaction time and the specific activity of the purified enzyme
260 was estimated to be about 16.0 U/g under the experimental conditions, comparable to
261 the values obtained for two enzymes purified from *C. gestroi* (6.2 and 7.6 U/g) [31].
262 rOfLPMO1 also oxidatively hydrolyzed β-chitin and produced a series of chitin
263 oligosaccharides in aldonic acid or lactone forms. The mass-to-charge ratio (*m/z*)
264 profiles of the digestion products in the mass spectral analysis consisted of oxidized
265 oligosaccharides with different degrees of polymerization (DP). The products
266 corresponding to even-numbered oligosaccharides with DP6 and DP8 had higher

intensities than the odd-numbered products with DP5 and DP7 (left panel in Fig. 3c). No oxidized product was detected either in the enzyme-omitted negative controls or in a reaction where micro-cellulose was used as the substrate (middle and right panels in Fig. 3c), suggesting LPMO1s are not involved in cellulose degradation. A potential synergistic effect between rOfLPMO1 and recombinant chitinase h (rOfChi-h) was examined using either α- or β-chitin as the substrate. As shown in Fig. 3c and Table 1, a mixture of rOfLPMO1 and rOfChi-h generated more reducing sugar from both substrates than the sum generated from reactions catalyzed by individual enzymes, indicating that there is a synergistic effect in chitin degradation between LPMO1 and chitinase h.

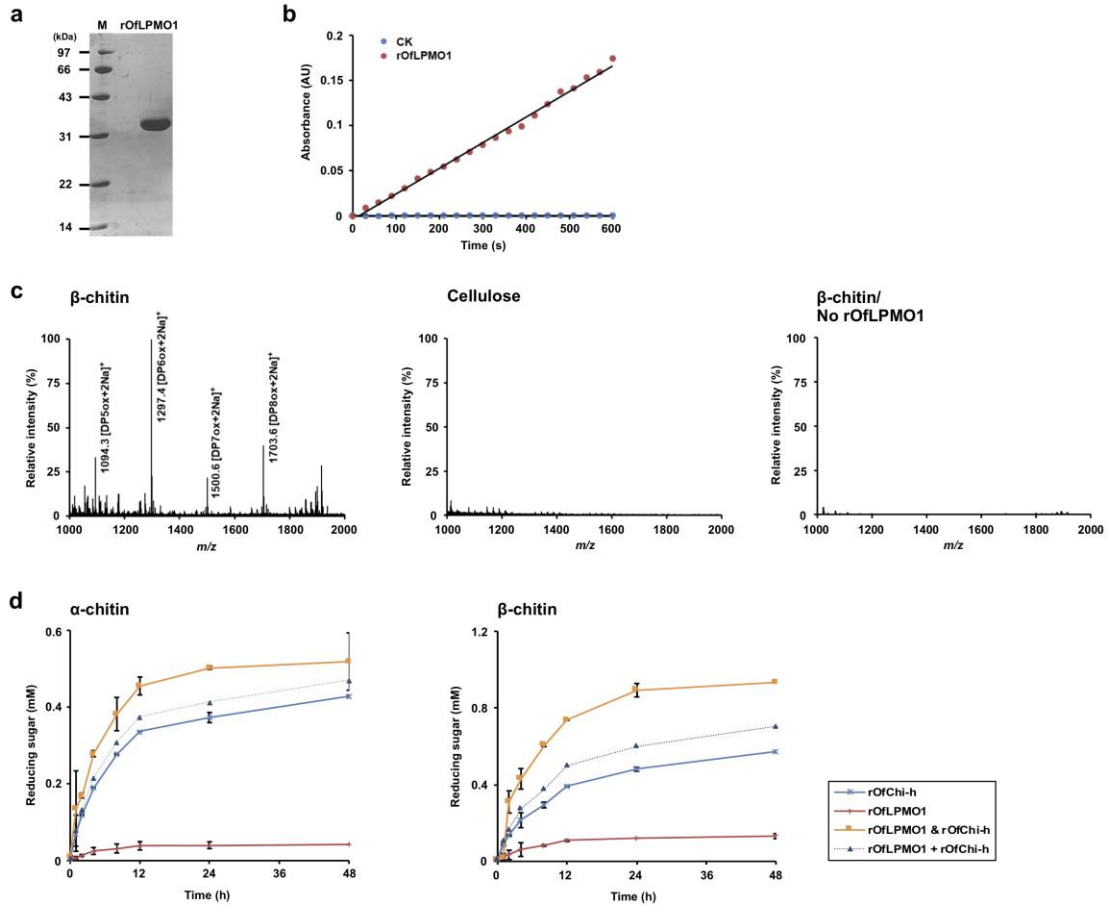

Fig. 3 Enzymatic properties of rOfLPMO1. a SDS-PAGE analysis. rOfLPMO1

279 protein obtained by β-chitin bead affinity chromatography was subjected to
280 electrophoresis on a 15% SDS-PAGE and stained with Coomassie Brilliant Blue
281 R-250. **b** Enzymatic activity. rOfLPMO1 (1 μM) was incubated with 5 mM 2, 6-DMP
282 and 100 μM H_2O_2 in 100 mM sodium phosphate (pH 6.0) at 30°C. The absorbance at
283 469 nm was measured every 30 s up to 600 s (red dots). The same assay without
284 rOfLPMO1 was performed as a negative control (blue dots). **c** LPMO substrate
285 specificity testing with β-chitin and cellulose. rOfLPMO1 (1 μM) was incubated with 2
286 mg/ml β-chitin (left panel) or microcrystalline cellulose (middle panel) in 20 mM
287 sodium phosphate buffer (pH 6.0) containing 1 mM ascorbic acid at 30°C for 24 h
288 followed by centrifugation at 17,000 x g. The supernatants were analyzed by
289 MALDI-TOF/TOF mass spectrometry. The same assay with β-chitin without
290 rOfLPMO1 was performed as a negative control (right panel). **d** The synergistic effect
291 between rOfLPMO1 and rOfChi-h. "rOfLPMO1 + rOfChi-h" indicates the calculated
292 sum of the reducing sugar generated by the individual enzymes. The "rOfLPMO1 &
293 rOfChi-h" indicates the reducing sugar produced by combining these two enzymes in
294 the reaction. Left panel: α-chitin as the substrate; Right panel: β-chitin as the substrate.
295
296 **Table 1.** The synergistic effect between rOfLPMO1 and rOfChi-h.

Substrate	Activity* (μmol/min)				Synergism coefficient
	rOfLPMO1	rOfChi-h	rOfLPMO1 & rOfChi-h	rOfLPMO1 + rOfChi-h	
α-chitin	0.11 ± 0.02	1.00 ± 0.02	1.41 ± 0.05	1.11	1.27
β-chitin	0.28 ± 0.20	1.13 ± 0.02	2.58 ± 0.48	1.41	1.83

297 *Activity was calculated at 2 h after incubation.

298 "rOfLPMO1 + rOfChi-h" indicates the calculated sum of the reducing sugar generated by the
299 individual enzymes. "rOfLPMO1 & rOfChi-h" indicates the reducing sugar produced by
300 combining these two enzymes in the same reaction.
301 Synergism coefficient = activity (rOfLPMO1 & rOfChi-h)/(activity rOfLPMO1 + activity
302 rOfChi-h)

303 **Effect of RNAi for *TcLPMO1* and *LmLPMO1* on insect molting and survival**

304 Double-stranded RNA (dsRNA)-mediated transcript down-regulation (RNAi) was
305 performed to determine the role of *TcLPMO1* and *LmLPMO1* in development and
306 molting of *T. castaneum* and *L. migratoria*, respectively. To analyze the transcript
307 abundance for each *LPMO1* gene after RNAi, real-time PCR experiments were carried
308 out. Injection of dsRNA for *TcLPMO1* (ds*TcLPMO1*) into the last instar larvae led to a
309 substantial depletion of *TcLPMO1* transcripts at the young pupal stage (day 1 pupae)
310 (Supplementary Fig. 3a) when the targeted gene is maximally expressed (see Fig. 2b).
311 Similarly, injection of ds*LmLPMO1* into the 5th instar day 1 nymphs caused a
312 substantial decrease in the level of *LmLPMO1* transcripts (Supplementary Fig. 3b).

313 In *T. castaneum*, injection of ds*TcLPMO1* into early instar larvae had no effect on
314 the subsequent molt and the resulting penultimate instar larvae developed normally
315 (Fig. 4a). However, all of the larvae failed to complete the molt to the last larval instar
316 (phenotype 1 in Fig. 4a). Slippage of the old larval cuticle was observed, but the
317 penultimate instar larvae were trapped inside the old cuticle and died. When
318 penultimate instar larvae were treated with ds*TcLPMO1*, the insects molted normally to
319 the last instar larvae, but they subsequently failed to complete the larval-pupal molt and

died as pharate pupae entrapped in the old larval cuticle (Phenotype 2 in Fig. 4a). When ds*TcLPMO1* was injected into last instar larvae, developmental arrest occurred during the pupal-adult molt when the pharate adults became entrapped in their pupal cuticle. Pupal cuticle slippage was evident, but the insects were unable to shed the pupal exuvium and died (Phenotype 3 in Fig. 4a). Similarly, injection of ds*TcLPMO1* into day 0 pupae also caused an incomplete pupal-adult molting in all of the insects (Phenotype 3 in Fig. 4a). These results indicate that TcLPMO1 is required for all types of molting (larval-larval, larval-pupal and pupal-adult) in *T. castaneum*.

In contrast, injection of ds*LmLPMO1* into the 5^{th} instar day 1 nymphs resulted in terminal developmental arrest. Approximately 10% of the nymphs died without dorsal splitting (Phenotype 1 in Fig. 4b), while ~70% of the nymphs initiated a molting process exhibiting both a dorsal split and new adult cuticle. However, the insects failed to shed the antecedent cuticle and died (Phenotype 2 in Fig. 4b). All of these results suggest that insect LPMO1 appears to play an essential role during the molting process, presumably in turnover of cuticle chitin, which is critical for completion of the molt. To evaluate this hypothesis, we further analyzed by TEM the ultrastructure of cuticles from TcLPMO1- and LmLPMO1-deficient insects.

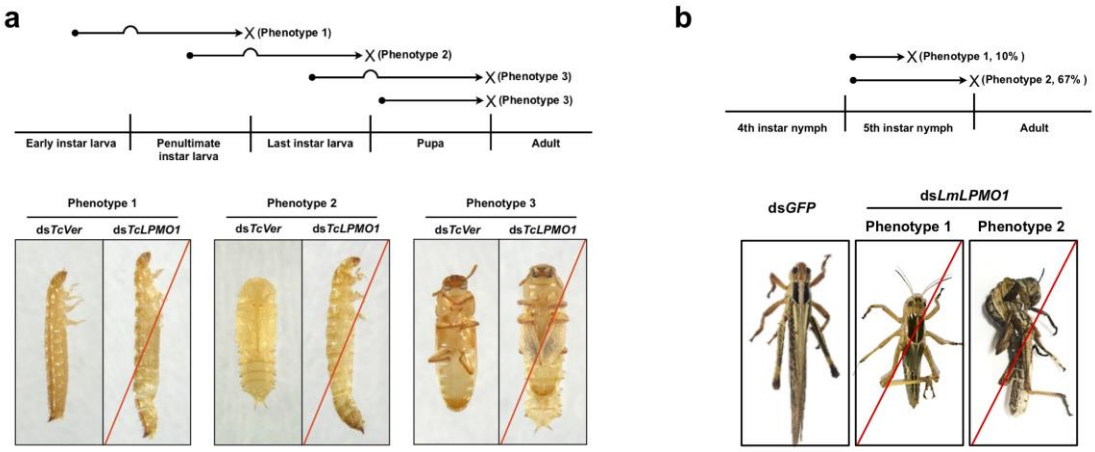

337

338 **Fig. 4 Lethal phenotypes produced by RNAi for *LPMO1* in *T. castaneum* and *L.***

339 ***migratoria*. a** In *T. castaneum*, injection of ds*TcLPMO1* (200 ng per insect) into early

340 instar, penultimate and last instar larvae had no effect on their subsequent molts and the

341 resulting insects developed normally. However, they failed to undergo penultimate-last

342 instar larval (Phenotype 1), larval-pupal (Phenotype 2) and pupal-adult (Phenotype 3)

343 molts, respectively, and died entrapped in their exuviae (red lines). A similar

344 pupal-adult molting defect was also obtained when ds*TcLPMO1* was injected into day

345 0 pupae. **b** In *L. migratoria*, injection of ds*LmLPMO1* (10 µg per insect; injected twice)

346 into 5th instar day 1 (first injection) and day 3 (second injection) nymphs resulted in

347 developmental arrest and death (red lines) without dorsal splitting (Phenotype 1, ~10%)

348 or exhibiting a dorsal splitting during the molt but entrapped in their nymphal cuticle

349 (Phenotype 2, ~70%).

350

351 **Ultrastructure of cuticles from LPMO1-deficient insects**

352 Because loss of function of *LPMO1* by RNAi caused molting arrests in both *T.*

353 *castaneum* and *L. migratoria*, we analyzed by TEM the morphology and ultrastructure

354 of the old and newly forming cuticles during molting periods in both species. In *T.*

castaneum, there were no obvious differences in morphology of the newly forming body wall cuticles of ds*TcLPMO1*-treated insects isolated at the penultimate larval instar, pharate pupal and pharate adult stages when compared with the ds*TcVer*-treated controls. New cuticles from both control and TcLPMO1-depleted insects exhibited well-organized, horizontal alternating electron-dense and electron-lucent chitinous laminae, as well as vertically oriented helicoidal pore canals in the larval and pupal cuticles or wide vertical structures with a central chitin fiber core of pore canal fibers (PCFs) in the adult cuticle (bottom panels in Fig. 5a-c). In the old cuticles at each molting stage analyzed, the endocuticles of ds*TcVer*-treated controls had been degraded (top left panels in Fig. 5a-c). In contrast, RNAi for *TcLPMO1* resulted in failure of turnover of the endocuticular layer in which the horizontal chitinous laminae and vertical pore canals remained essentially intact (top right panels in Fig. 5a-c).

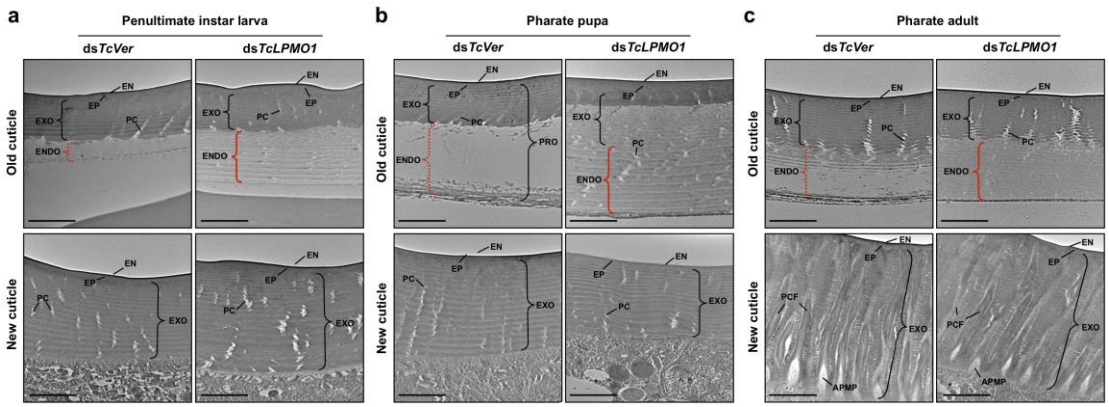

Fig. 5 Ultrastructure of cuticles from TcLPMO1-deficient larvae, pharate pupae and pharate adults of *T. castaneum*. Ultrastructure of old (top panels) and newly forming cuticles (bottom panels) from penultimate instar larvae **a**, pharate pupae **b** and pharate adults **c** that had been injected with ds*TcLPMO1* or ds*TcVer* at early instar, penultimate and last instar larval stages, respectively, was analyzed by TEM.

373 ds*TcVer*-treated controls showed degradation of the endocuticle (ENDO) in the
374 overlying old cuticle (red dotted brackets) during each molt analyzed, while those of
375 TcLPMO1-deficient insects were intact, retaining a number of chitinous horizontal
376 laminae (red solid brackets). EN, envelope; EP, epicuticle; EXO, exocuticle; ENDO,
377 endocuticle; PC, pore canal; PCF, pore canal fiber; APMP, apical plasma membrane
378 protrusion. Scale bar = 2 μm.

379 To investigate the functional importance of *LmLPMO1* in turnover/morphology of
380 the old and/or new cuticles during adult eclosion in *L. migratoria*, those tissues were
381 dissected from the third abdominal segment of pharate adults (5^{th} instar day 9 nymphs)
382 that had been injected with ds*GFP* (control) or ds*LmLPMO1* on 5^{th} instar day 1 and
383 again on day 3. Paraffin sections of tissues stained with hematoxylin and eosin showed
384 that the old cuticle of ds*LmLPMO1*-treated insects was much thicker than that of
385 ds*GFP*-treated controls (Fig. 6a), suggesting that LmLPMO1-deficient insects might
386 have failed to digest the old cuticle. To confirm that the turnover of the old cuticle was
387 affected, we further performed TEM analysis of old and new cuticles. The endocuticle
388 portion of the old cuticle of ds*GFP*-control insects was nearly completely digested,
389 whereas that of ds*LmLPMO1*-treated insects appeared to be intact, retaining numerous
390 horizontal chitin laminae and vertical pore canals (left panels in Fig. 6b). As observed
391 with cuticles of *TcLPMO1*-depleted *T. castaneum*, RNAi for *LmLPMO1* yielded no
392 obvious differences in morphology of either the horizontal laminae or vertical pore
393 canals in the newly formed adult cuticle compared with that of the ds*GFP*-control (right
394 panels in Fig. 6a). All of these results indicate that LPMO1 plays a role during molting

in digestion of chitin in the old cuticle, which is critical for the completion of the molt, but not in the formation of new cuticle or its morphology including the chitinous laminar organization and pore canal/PCF structure in both *T. castaneum* and *L. migratoria*.

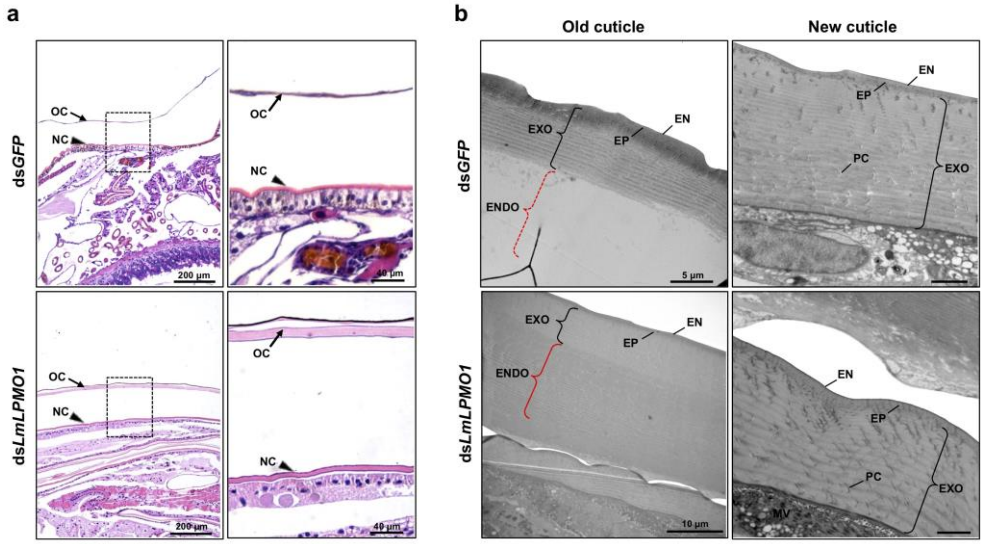

Fig. 6 Ultrastructure of cuticle from pharate adult of LmLPMO1-deficient *L. migratoria*. **a** Paraffin sections (5 μm) of third abdominal segments from pharate adults (5th instar day 9 nymphs) that had been injected with ds*LmLPMO1* or ds*GFP* as the 5th instar day 1 nymphs were stained with hematoxylin and eosin. Right panels show enlarged images of the old nymphal cuticle (OC) and newly forming adult cuticle (NC) (box in left panels). The OC of ds*LmLPMO1*-insects was significantly thicker than that of ds*GFP*-controls. **b** Ultrastructures of the old and new cuticles from each dsRNA-treated insect were analyzed by TEM. ds*GFP*-treated controls showed the degraded endocuticle (ENDO) in the overlying old cuticle (red dotted bracket in top left panel), while that of ds*LmLPMO1*-treated insects remained intact, exhibiting numerous

chitinous horizontal laminae (red solid bracket in left bottom panel). EN, envelope; EP, epicuticle; EXO, exocuticle; ENDO, endocuticle; PC, pore canal.

Discussion

The degradation of extracellular matrix polysaccharides in insects and plants presents special challenges because of the crystallinity and possible cross-linking of the substrates. A commonly held view envisaged that a combination of families of endo- and exo-acting hydrolytic enzymes could accomplish the digestion of recalcitrant polysaccharides including chitin and cellulose [32,33]. However, the relatively recent discovery that proteins collectively known as LPMOs, which bind to these substrates, promote utilization of insoluble substrates and have oxidase activities of their own, has provided new insight about the mechanism of turnover of naturally occurring polysaccharides by microbes as well as arthropods [8,12-16,25-27]. LPMOs from microbes break the C-H bond of either C1 or C4 carbons of polysaccharides using a peroxidase activity with H_2O_2 as the co-substrate resulting in aldonic acid or lactone products. This process results in the generation of internal entry sites in the polysaccharide for the hydrolytic enzymes such as chitinases and cellulases in addition to facilitating the decrystallization of chitin or cellulose chains from crystalline bundles [34].

Besides microbes, arthropods also contain a variety of LPMO-like proteins. Recently, analysis of the gut proteome and transcriptome of the ancient insect species, *T. domestica* from the order *Zygentoma*, has confirmed the expression in the gut of a large family of LPMOs belonging to the AA15 family of enzymes. These proteins

promote digestion of dietary crystalline cellulose without the assistance of gut microbes, unlike termite species that require such microbial assistance for cellulose digestion. Individual TdLPMOs differed in their ability to act on either chitin or cellulose or both. On the other hand, two LPMOs from the lower termite, *C. gestroi*, could act only on chitin and not on cellulose, indicating their role in structural matrix remodeling rather than in digestion. So far, the only evidence for the idea that LPMOs might have a role in insect cuticle turnover comes from genome-wide RNAi of *D. melanogaster* and the iBeetle project that identified pupal lethality and other defects in *T. castaneum* (http://ibeetle-base.uni-goettingen.de/). However, there have been no direct studies on chitin turnover in the cuticle or on the enzymatic activity/specificity of LPMO-like proteins in these species. Our study addresses these specific issues and points to an essential role for these enzymes in chitin turnover, which is not met alone by the assortment of endo- and exochitinases.

The nine TcLPMO homologs and other LPMO-like proteins deduced from 12 insect genomes obtained with TdLPMO as query are distributed into at least four distinct branches and display unusual properties. There is only one representative from each insect species in LPMO groups I and II, which have distinctly different protein domain compositions. All group I proteins have two copies of a 6-cysteine repeat often associated with chitin-binding domains. However, these cysteine repeats are not related to the CBM14 domains present in insect chitinase-like proteins [35]. Group II LPMOs lack this domain but have a predicted C-terminal transmembrane domain. Group III proteins in several insect genomes contain redundant enzymes that have only the AA15

454 catalytic domain. Group IV proteins have an interesting distribution among insects,
455 being prevalent only in lepidopteran species. The significance of their unique
456 distributions remains unknown. The presence of these distinct groups among insect
457 species suggests functional differences among them. This inference is further supported
458 by the limited data that we currently have on tissue specificity of expression of these
459 LPMO groups. Groups I and II enzymes from both *T. castaneum* and *L. migratoria* are
460 expressed predominantly in the epidermis but not in the midgut, suggesting their
461 involvement in chitin remodeling in the cuticle rather than a digestive function. They
462 are also expressed at comparable periods in the molt cycle and not in the adult stage. In
463 contrast, all seven group III enzymes from *T. castaneum* are expressed almost
464 exclusively in the gut and not in the carcass (Supplementary Fig. 4), suggesting their
465 involvement in digestion of dietary chitin and/or peritrophic matrix-associated chitin,
466 but not in cuticle chitin turnover.

467 We were able to express recombinantly the full-length OfLPMO1 protein from *O.*
468 *furnacalis*, which was also identified in our BlastP search. OfLPMO1 shares 71%
469 identity with the TcLPMO1 from *T. castaneum* and 63% identity with the LmLPMO1
470 from *L. migratoria* and also has the 12 cysteine-containing C-terminal motif. Besides
471 exhibiting peroxidase activity with 2,6-DMP as the substrate, the highly purified
472 enzyme oxidized crystalline α- and β-chitins, but not cellulose, yielding
473 chitooligosaccharide products consistent with a role in chitin turnover, but not in the
474 digestion of dietary cellulose, similar to TdAA15B of *T. domestica*. It should be
475 emphasized that besides sharing a high degree of amino acid sequence identity, the

476 three LPMO1 proteins from *T. castaneum, L. migratoria* and *O. furnacalis* have the
477 same four essential amino acids (H1, H91, A89 and F186) involved in the T-brace
478 structure containing the catalytic Cu atom first identified in the TdAA15B enzyme,
479 which is specific for chitin [8].

480 Finally, we demonstrated by RNAi that the LPMO1 enzymes in two different
481 insect orders are critical for insect molting as well as cuticle digestion. Administration
482 of dsRNA for the single copy of the gene encoding this enzyme resulted in molting
483 failure in *T. castaneum* at all developmental stages. In cases other than the pupal stage,
484 the insects managed to molt to the next developmental stage (larva, prepupa, or pupa)
485 but died without completing the next molt cycle due to a high level of transcript
486 depletion of the targeted gene. While we do not have a precise explanation for the delay
487 in the development of the phenotype until the next molt cycle, we hypothesize a delay
488 in protein depletion due to a long half-life of the LPMO protein past the point of
489 transcript depletion.

490 Our studies provide clear cut evidence that, compared to the control insects
491 showing dissolution of the old cuticle, following RNAi of just one of several *LPMO*
492 genes present in insect genomes, the laminar architecture of the old cuticle remains
493 mostly intact, even though the assortment of chitinolytic enzymes is produced normally.
494 Note that the LPMO-depleted insects do complete one molt cycle presumably utilizing
495 the chitinolytic enzymes. This report is the first demonstration of the essential role of an
496 LPMO in promoting the turnover of the chitinous cuticle. The failure to molt after
497 depletion of a single oxidative enzyme supports the hypothesis that LPMOs are as

498 equally important as the chitinolytic enzymes in the digestion of cuticle chitin at each
499 molt cycle. For applications in economic and medical entomology for the development
500 of novel insecticides, LPMOs may be potential targets identified via comparative and
501 functional insect genomics.

Material and Methods

Insects

The GA-1 strain of *T. castaneum* [36] was used for this study. Beetles were reared at 30°C and 50% relative humidity in whole wheat flour containing 5% brewer's yeast as described previously [37]. *L. migratoria* was kindly provided by the Institute of Zoology, Chinese Academy of Sciences (CAS). Nymphs were reared on fresh wheat sprouts in the laboratory at 28°C under a 14 h light/10 h dark diurnal cycle.

Cloning of *TcLPMO1, LmLPMO1* and *OfLPMO1* cDNAs

T. castaneum, *L. migratoria* and *O. furnacalis* homologs of TdAA15A from *T. domestica* (accession number: GASN01405718.1) were identified by performing a BLAST search of the *T. castaneum* genome and the *L. migratoria* and *O. furnacalis* transcriptomes. To clone *TcLPMO1* cDNA, total RNA was isolated from a pool of six whole *T. castaneum* pupae (mixture of day 0-5 pupae) by using the RNeasy Mini Kit (Qiagen). First strand cDNAs were synthesized with the Super Script III First-Strand Synthesis System (Invitrogen) using an oligo-$(dT)_{18}$ primer. To clone *LmLPMO1* and *OfLPMO1* cDNAs, total RNA was isolated from *L. migratoria* 5^{th} instar day 1 nymphs and *O. furnacalis* pharate pupae, respectively, using Trizol reagent (Invitrogen), and then treated with DNase I (Takara). First strand cDNAs were synthesized using the Reverse Transcriptase M-MLV (Takara) and used as template for cDNA amplification. cDNAs containing the predicted full-length coding sequence of *TcLPMO1*, *LmLPMO1* and *OfLPMO1* were amplified by PCR using the gene-specific primers shown in

Supplementary Table 1. The cDNA fragments were cloned into pGEM-T (Promega) or pEASY-T1 vector (TransGen Biotech) and sequenced. GenBank accession numbers of the TcLPMO1, LmLPMO1 and OfLPMO1 clones are MZ636451, MZ440879 and MZ440880, respectively.

Protein sequence and phylogenetic analysis

LPMO-like proteins in fully sequenced or well annotated insect genomes/transcriptomes were identified by a BLAST search of the NCBI database using the TdAA15A protein sequence as the query. Multiple sequence alignment of proteins was carried out using the ClustalW software tool (https://www.genome.jp/tools-bin/clustalw). SignalP-5.0 (http://www.cbs.dtu.dk/services/SignalP/) was used to predict signal peptides. LPMO domains were identified using the Conserved Domain Database (CDD, https://www.ncbi.nlm.nih.gov/cdd). A core region of homologous sequence highly conserved in all LPMO1 proteins analyzed, including an LPMO domain and a C-terminal cysteine-rich domain, was aligned. A phylogenetic tree was constructed with the MEGA 7 program [38] using the neighbor-joining method. See Supplementary Table 2 for the accession numbers of LPMO1 proteins used for amino acid sequence alignment and phylogenetic analysis.

Gene expression analysis by real-time PCR

To analyze temporal and spatial expression patterns of *TcLPMO1* and *LmLPMO1*, total RNA was isolated from embryos, young larvae, old larvae, pharate pupae, pupae and adults, larval midgut and carcass (whole body without midgut) of *T. castaneum*; and epidermis of 4^{th} instar day 5, 5^{th} instar day 1, 3, 5 and 7 and adult day 1; and midgut, testis and ovarian tissues dissected from 5^{th} instar day 3 of *L. migratoria*. For *TcLPMO1*, real-time PCR was done in a 40 µl reaction volume containing 1 µl of template cDNA, 20 µl TB Green Premix Ex Taq (TAKARA), 0.25 µM of each primer using the Thermal Cycler Dice real-time PCR system III (TAKARA). For *LmLPMO1*, real-time PCR was performed in a 20 µL reaction volume containing 10 µL TransStart Top Green qPCR SuperMix (Trans), 2 µL template cDNA and 0.2 µM of each primer using the Real-time PCR Detection System LightCycler480II (Roche). Transcript levels of the *T. castaneum* ribosomal protein S6 (*TcRpS6*) or *L. migratoria* ribosomal protein 49 (*LmRp49*) were measured to normalize for differences among the concentrations of cDNA templates. Each sample included three biological replicates and three technical replicates. The relative expression levels for each gene were calculated relative to the reference gene according to the $2^{-\Delta\Delta Ct}$ method [39]. See Supplementary Table 1 for the primer sequences used for real-time PCR experiments.

Expression of recombinant *Of*LPMO1 protein

The coding sequence excluding the putative signal peptide of *Of*LPMO1 was optimized to the yeast codon bias for yeast expression, synthesized the DNA template (Taihe Biotechnology) and used for PCR amplification using the primer set: 5´-AGA

AGG GGT ATC TCT CGA GAA AAG ACA TGG AAG ATT GAT GGA CCC-3´ and 5´-GAA TTA ATT CGC GGC CGC TTA GTA ACA CCT ACA CCT GT-3´. The forward and reverse primers contain *Xho I* and *Not I* recognition sites (underlined), respectively, to facilitate directional cloning into the pPIC9 vector (Invitrogen). The PCR product was digested with *Xho I* and *Not I* and subcloned into the same sites of the pPIC9 plasmid DNA behind the signal cleavage site with α-factor at the N-terminus in frame. The recombinant plasmid was linearized using *Sac I* and then transformed into *Pichia pastoris* strain GS115. Positive clones were selected and the recombinant OfLPMO1 protein (rOfLPMO1) was obtained by induction with 1% methanol for 120 h. rOfLPMO1 was purified by 75% saturation of ammonium sulfate precipitation, followed by affinity chromatography using β-chitin beads as described previously [40]. The purity of affinity-purified rOfLPMO1 was analyzed by 15% SDS-PAGE.

Enzyme assay

Enzymatic activity of the purified rOfLPMO1 was measured by utilizing the peroxidase activity associated with this class of enzymes using 2,6-dimethoxyphenol (2,6-DMP) and H_2O_2 as co-substrates [41] with modifications. The reaction solution containing 5 mM 2,6-DMP and 100 µM H_2O_2 in 200 µl of 100 mM sodium phosphate (pH 6.0) was preincubated at 30°C for 10 min, and then the absorbance at 469 nm was measured every 30 s shortly after adding rOfLPMO1 (final concentration of 5 µM). In the control group, the reaction solution contained the same components except that no

589 enzyme was added. For determination of activity of rOfLPMO1 toward chitin and
590 cellulose, rOfLPMO1 (5 μM) was incubated with 2 mg/ml β-chitin or microcrystalline
591 cellulose (Sigma) in 300 μl of 20 mM sodium phosphate buffer (pH 6.0) containing 1
592 mM ascorbic acid at 30°C for 24 h with rotation. The reaction mixture was
593 centrifuged at 17,000 x g for 10 min and 0.5 μL of the reaction product in the
594 supernatant was analyzed by MALDI-TOF/TOF mass spectrometry (Waters).
595 Both α-chitin and β-chitin were used to detect the synergistic effect (if any)
596 between rOfLPMO1 and recombinant OfChi-h (rOfChi-h). For the single enzyme
597 hydrolysis condition, a final concentration of 1 μM rOfChi-h or 5 μM rOfLPMO1 was
598 added in a total volume of 1.0 mL containing 100 mM sodium phosphate buffer (pH 6.0)
599 and 2 mg/mL chitin in a 2 mL Eppendorf tube. For the two-enzyme combination
600 condition, 1 μM rOfChi-h and 5 μM rOfLPMO1 were added to the reaction system
601 together. In addition, 1 mM ascorbic acid was added to the reaction mixture whenever
602 LPMO was included in the assay. These tubes were incubated horizontally in an
603 incubator at 200 rpm for 48 h at 30°C. A 0.06 mL sample was withdrawn from
604 well-mixed digestion mixtures at selected time-points during digestions. An aliquot of
605 0.18 mL potassium ferriferrocyanide (2 mg/mL) was then added and the mixture was
606 boiled for 15 min. The amount of reducing sugar generated corresponded to the
607 potassium ferriferrocyanide consumption, which was quantified by measuring the
608 absorbance at 420 nm. All the assays were performed in triplicate.
609
610 **RNA interference (RNAi)**

611 Templates for synthesis of double-stranded RNA (dsRNA) for *TcLPMO1*
612 (ds*TcLPMO1*) and *LmLPMO1* (ds*LmLPMO1*) were amplified by PCR using the
613 gene-specific primers containing T7 RNA promoter sequences at the 5′-ends. dsRNAs
614 were synthesized and purified according to the protocol described previously [42,43]. In *T.*
615 *castaneum*, ds*TcLPMO1* (200 ng per insect) was injected into early instar larvae,
616 penultimate instar larvae, last instar larvae or day 0 pupae (n = 20-40 for each of the
617 three independent experiments). To analyze knockdown levels of *TcLPMO1* transcripts,
618 total RNA was isolated from whole day 1 pupae (n = 3) that had been injected with
619 dsRNA at last instar larval stage. In *L. migratoria*, ds*LmLPMO1* (10 μg per insect) was
620 injected into the 5th instar day 1 nymphs (1st injection), and the same amount of dsRNA
621 was injected a second time 3 d after the first injection to increase RNAi efficiency (n =
622 10 for each of the three independent experiments). To analyze knockdown levels of
623 *LmLPMO1* transcripts, total RNA was isolated from the epidermis of 5th instar day 5
624 nymphs (2 d after 2nd dsRNA injection). dsRNAs for *T. castaneum Vermilion*
625 (ds*TcVer*) and green fluorescent protein (ds*GFP*) were synthesized as described
626 previously [43,44] and injected to serve as a negative control for *T. castaneum* and *L.*
627 *migratoria,* respectively. The primer sequences used and lengths of the dsRNAs are
628 listed in Supplementary Table 1.
629
630 **Histochemistry**
631 *L. migratoria* pharate adults (5th instar day 9 nymphs) that had been injected with
632 ds*LmLPMO1* or ds*GFP* into 5th instar day 1 nymphs were collected, and their third

633 abdominal segments were dissected. Samples were fixed in 4% paraformaldehyde for
634 24 h, dehydrated in an ethanol gradient of 30, 50, 70, 90 and 100% for 30 min each, and
635 then embedded in paraffin. Paraffin sections (5 μm) were stained with hematoxylin and
636 eosin (Beyotime Biotechnology) and then observed using the Olympus IX-83 inverted
637 microscope.
638
639 **Transmission electron microscopy (TEM)**
640 Penultimate instar larvae, pharate pupae (day 2 prepupae) and pharate adults (day 5
641 pupae) of *T. castaneum* that had been treated previously with ds*TcLPMO1* or ds*TcVer*
642 were collected and fixed in a mixture of 4% paraformaldehyde and 0.1%
643 glutaraldehyde in 0.1 M sodium cacodylate buffer (pH 7.4) for 24 h at room
644 temperature. Ultrastructure of cuticles from the dsRNA-treated animals was analyzed
645 by TEM as described previously [45]. In the case of samples of *L. migratoria*, pharate
646 adults (5th instar day 9 nymphs) that had been injected with ds*LmLPMO1* or ds*GFP* at
647 the 5th instar day 1 nymph stage were collected, and the epidermis of their third
648 abdominal segments were dissected and fixed in a mixture of 4% paraformaldehyde
649 and 0.1% glutaraldehyde in 0.1 M phosphate buffer (pH7.4) for 24 h at room
650 temperature. Samples were washed with 0.1 M phosphate buffer, and then fixed with 1%
651 osmium tetroxide for 3 h. The tissues were rinsed with phosphate buffer, dehydrated in
652 acetone, and then embedded in Epon 812 (Sigma) for 2 h at room temperature and
653 baked in a 62°C oven for 48 h, followed by ultrathin sectioning. Ultrathin sections

were stained with 4% aqueous uranyl acetate for 10 min and then imaged using the JEM-1200EX transmission electron microscope (JEOL).

Acknowledgements

This work was supported by the National Natural Science Foundation of China (31872972，31830076), the Shenzhen Science and Technology Program (Grant No. KQTD20180411143628272), National Research Foundation of Korea (NRF) grant funded by the Korean government (MSIT) (NRF-2018R1A2B6005106 and NRF-2021R1A2C1006645) and Basic Science Research Program through the NRF funded by the Ministry of Education (NRF-2020R1I1A3066074).

Competing interests

The authors declare that no competing interests exist.

Author contributions

Q.Y., and Y.A. supervised the project. Q.Y. and Y.A. designed the research study. M.Q., M.K., X. D., X.G., S.T., S.G.M. and M.Y.N. performed the experiments. M.Q., M.K., X. D., X.G., S.T., S.G.M., M.Y.N., K.J.K., S.M. and Y.A. analyzed data and discussed results. Q.Y. and Y.A. wrote the manuscript. All authors reviewed the manuscript.

References

1 Locke, M. The wigglesworth lecture: Insects for studying fundamental problems in biology. *Journal of Insect Physiology* **47**, 495-507, doi:10.1016/s0022-1910(00)00123-2 (2001).

2 Moussian, B., Seifarth, C., Muller, U., Berger, J. & Schwarz, H. Cuticle differentiation during *Drosophila* embryogenesis. *Arthropod Structure & Development* **35**, 137-152, doi:10.1016/j.asd.2006.05.003 (2006).

3 Noh, M. Y., Muthukrishnan, S., Kramer, K. J. & Arakane, Y. Development and ultrastructure of the rigid dorsal and flexible ventral cuticles of the elytron of the red flour beetle, *Tribolium castaneum*. *Insect Biochemistry and Molecular Biology* **91**, 21-33, doi:10.1016/j.ibmb.2017.11.003 (2017).

4 Muthukrishnan, S., Merzendorfer, H., Arakane, Y. & Kramer, K. J. in *Insect Molecular Biology and Biochemistry* Ch. 7, 193-235 (Academic Press, 2012).

5 Muthukrishnan, S., Merzendorfer, H., Arakane, Y. & Yang, Q. Chitin Organizing and Modifying Enzymes and Proteins Involved In Remodeling of the Insect Cuticle. *Adv Exp Med Biol* **1142**, 83-114, doi:10.1007/978-981-13-7318-3_5 (2019).

6 Zhu, K. Y., Merzendorfer, H., Zhang, W., Zhang, J. & Muthukrishnan, S. Biosynthesis, turnover, and functions of chitin in insects. *Annual Review of Entomology* **61**, 177-196, doi:10.1146/annurev-ento-010715-023933 (2016).

7 Chylenski, P. *et al.* Lytic polysaccharide monooxygenases in enzymatic processing of lignocellulosic biomass. *ACS Catalysis* **9**, 4970-4991, doi:10.1021/acscatal.9b00246 (2019).

8 Sabbadin, F. *et al.* An ancient family of lytic polysaccharide monooxygenases with roles in arthropod development and biomass digestion. *Nature Communications* **9**, 756, doi:10.1038/s41467-018-03142-x (2018).

9 Forsberg, Z. *et al.* Polysaccharide degradation by lytic polysaccharide monooxygenases. *Current Opinion in Structural Biology* **59**, 54-64, doi:10.1016/j.sbi.2019.02.015 (2019).

10 Agostoni, M., Hangasky, J. A. & Marletta, M. A. Physiological and molecular understanding of bacterial polysaccharide monooxygenases. *Microbiology and Molecular Biology Reviews* **81**, doi:10.1128/MMBR.00015-17 (2017).

11 Langston, J. A. *et al.* Oxidoreductive cellulose depolymerization by the enzymes cellobiose dehydrogenase and glycoside hydrolase 61. *Applied and Environmental Microbiology* **77**, 7007-7015, doi:10.1128/AEM.05815-11 (2011).

12 Vaaje-Kolstad, G. *et al.* An oxidative enzyme boosting the enzymatic conversion of recalcitrant polysaccharides. *Science* **330**, 219-222, doi:10.1126/science.1192231 (2010).

13 Hemsworth, G. R., Henrissat, B., Davies, G. J. & Walton, P. H. Discovery and characterization of a new family of lytic polysaccharide monooxygenases. *Nature Chemical Biology* **10**, 122-126, doi:10.1038/nchembio.1417 (2014).

14 Lo Leggio, L. *et al.* Structure and boosting activity of a starch-degrading lytic polysaccharide monooxygenase. *Nature Communications* **6**, 5961, doi:10.1038/ncomms6961 (2015).

15 Couturier, M. *et al.* Lytic xylan oxidases from wood-decay fungi unlock biomass degradation. *Nature Chemical Biology* **14**, 306-310, doi:10.1038/nchembio.2558 (2018).

16 Filiatrault-Chastel, C. *et al.* AA16, a new lytic polysaccharide monooxygenase family identified in fungal secretomes. *Biotechnology for Biofuels* **12**, 55, doi:10.1186/s13068-019-1394-y (2019).

17 Lombard, V., Golaconda Ramulu, H., Drula, E., Coutinho, P. M. & Henrissat, B. The

carbohydrate-active enzymes database (CAZy) in 2013. *Nucleic Acids Research* **42**, D490-495, doi:10.1093/nar/gkt1178 (2014).

18 Sabbadin, F. *et al.* Secreted pectin monooxygenases drive plant infection by pathogenic oomycetes. *Science* **373**, 774-779, doi:10.1126/science.abj1342 (2021).

19 Vaaje-Kolstad, G., Horn, S. J., van Aalten, D. M., Synstad, B. & Eijsink, V. G. The non-catalytic chitin-binding protein CBP21 from *Serratia marcescens* is essential for chitin degradation. *Journal of Biological Chemistry* **280**, 28492-28497, doi:10.1074/jbc.M504468200 (2005).

20 Vaaje-Kolstad, G. *et al.* Characterization of the chitinolytic machinery of *Enterococcus faecalis* V583 and high-resolution structure of its oxidative CBM33 enzyme. *Journal of Molecular Biology* **416**, 239-254, doi:10.1016/j.jmb.2011.12.033 (2012).

21 Bennati-Granier, C. *et al.* Substrate specificity and regioselectivity of fungal AA9 lytic polysaccharide monooxygenases secreted by *Podospora anserina*. *Biotechnology for Biofuels* **8**, 90, doi:10.1186/s13068-015-0274-3 (2015).

22 Fanuel, M. *et al.* The *Podospora anserina* lytic polysaccharide monooxygenase *Pa*LPMO9H catalyzes oxidative cleavage of diverse plant cell wall matrix glycans. *Biotechnology for Biofuels* **10**, 63, doi:10.1186/s13068-017-0749-5 (2017).

23 Isaksen, T. *et al.* A C4-oxidizing lytic polysaccharide monooxygenase cleaving both cellulose and cello-oligosaccharides. *Journal of Biological Chemistry* **289**, 2632-2642, doi:10.1074/jbc.M113.530196 (2014).

24 Vu, V. V. & Marletta, M. A. Starch-degrading polysaccharide monooxygenases. *Cellular and Molecular Life Sciences* **73**, 2809-2819, doi:10.1007/s00018-016-2251-9 (2016).

25 Aachmann, F. L., Sørlie, M., Skjåk-Bræk, G., Eijsink, V. G. H. & Vaaje-Kolstad, G. NMR structure of a lytic polysaccharide monooxygenase provides insight into copper binding, protein dynamics, and substrate interactions. *Proceedings of the National Academy of Sciences of the United States of America* **109**, 18779, doi:10.1073/pnas.1208822109 (2012).

26 Agger, J. W. *et al.* Discovery of LPMO activity on hemicelluloses shows the importance of oxidative processes in plant cell wall degradation. *Proceedings of the National Academy of Sciences of the United States of America* **111**, 6287-6292, doi:10.1073/pnas.1323629111 (2014).

27 Frandsen, K. E. *et al.* The molecular basis of polysaccharide cleavage by *lytic polysaccharide monooxygenases*. *Nature Chemical Biology* **12**, 298-303, doi:10.1038/nchembio.2029 (2016).

28 Franco Cairo, J. P. L. *et al.* On the roles of AA15 lytic polysaccharide monooxygenases derived from the termite Coptotermes gestroi. *Journal of inorganic biochemistry* **216**, 111316, doi:10.1016/j.jinorgbio.2020.111316 (2020).

29 Garcia-Gonzalez, E. *et al. Paenibacillus larvae* chitin-degrading protein *Pl*CBP49 is a key virulence factor in American Foulbrood of honey bees. *PLOS Pathogens* **10**, e1004284, doi:10.1371/journal.ppat.1004284 (2014).

30 Chiu, E. *et al.* Structural basis for the enhancement of virulence by viral spindles and their in vivo crystallization. *Proceedings of the National Academy of Sciences of the United States of America* **112**, 3973, doi:10.1073/pnas.1418798112 (2015).

31 Franco Cairo, J. P. L. *et al.* On the roles of AA15 *lytic polysaccharide monooxygenases* derived from the termite *Coptotermes gestroi*. *J Inorg Biochem* **216**, 111316, doi:10.1016/j.jinorgbio.2020.111316 (2021).

32 Jalak, J., Kurasin, M., Teugjas, H. & Valjamae, P. Endo-exo synergism in cellulose hydrolysis revisited. *Journal of Biological Chemistry* **287**, 28802-28815, doi:10.1074/jbc.M112.381624

(2012).
33 Qu, M. *et al.* High-speed atomic force microscopy reveals factors affecting the processivity of chitinases during interfacial enzymatic hydrolysis of crystalline chitin. *ACS Catalysis* **10**, 13606-13615, doi:10.1021/acscatal.0c02751 (2020).
34 Eibinger, M., Sattelkow, J., Ganner, T., Plank, H. & Nidetzky, B. Single-molecule study of oxidative enzymatic deconstruction of cellulose. *Nature Communications* **8**, 894, doi:10.1038/s41467-017-01028-y (2017).
35 Tetreau, G. *et al.* Analysis of chitin-binding proteins from *Manduca sexta* provides new insights into evolution of peritrophin A-type chitin-binding domains in insects. *Insect Biochemistry and Molecular Biology* **62**, 127-141, doi:10.1016/j.ibmb.2014.12.002 (2015).
36 Haliscak, J. P. & Beeman, R. W. Status of malathion Rresistance in five genera of beetles infesting farm-stored corn, wheat, and oats in the United States. *Journal of Economic Entomology* **76**, 717-722, doi:10.1093/jee/76.4.717 (1983).
37 Beeman, R. W. & Stuart, J. J. A gene for lindane + cyclodiene resistance in the red flour beetle (Coleoptera: Tenebrionidae). *Journal of Economic Entomology* **83**, 1745-1751, doi:10.1093/jee/83.5.1745 (1990).
38 Kumar, S., Stecher, G. & Tamura, K. MEGA7: molecular evolutionary genetics analysis version 7.0 for bigger datasets. *Molecular Biology and Evolution* **33**, 1870-1874, doi:10.1093/molbev/msw054 (2016).
39 Pfaffl, M. W. A new mathematical model for relative quantification in real-time RT–PCR. *Nucleic Acids Research* **29**, e45-e45, doi:10.1093/nar/29.9.e45 (2001).
40 Vaaje-Kolstad, G., Houston, D. R., Riemen, A. H., Eijsink, V. G. & van Aalten, D. M. Crystal structure and binding properties of the *Serratia marcescens* chitin-binding protein CBP21. *Journal of Biological Chemistry* **280**, 11313-11319, doi:10.1074/jbc.M407175200 (2005).
41 Breslmayr, E. *et al.* A fast and sensitive activity assay for lytic polysaccharide monooxygenase. *Biotechnology for Biofuels* **11**, 79, doi:10.1186/s13068-018-1063-6 (2018).
42 Arakane, Y. *et al.* The *Tribolium chitin synthase* genes *TcCHS1* and *TcCHS2* are specialized for synthesis of epidermal cuticle and midgut peritrophic matrix. *Insect Molecular Biology* **14**, 453-463, doi:10.1111/j.1365-2583.2005.00576.x (2005).
43 Zhao, X. *et al.* Mucin family genes are essential for the growth and development of the migratory locust, *Locusta migratoria*. *Insect Biochemistry and Molecular Biology,* **123**, 103404, doi:10.1016/j.ibmb.2020.103404 (2020).
44 Arakane, Y. *et al.* Molecular and functional analyses of amino acid decarboxylases involved in cuticle tanning in *Tribolium castaneum*. *Journal of Biological Chemistry* **284**, 16584-16594, doi:10.1074/jbc.M901629200 (2009).
45 Noh, M. Y. *et al.* Two major cuticular proteins are required for assembly of horizontal laminae and vertical pore canals in rigid cuticle of *Tribolium castaneum*. *Insect Biochemistry and Molecular Biology* **53**, 22-29, doi:10.1016/j.ibmb.2014.07.005 (2014).

Additional data files

Supplementary Table 1. Primers used for cloning, real-time PCR and dsRNA synthesis.

Supplementary Table 2. Accession numbers of insect LMPO1s used for the amino acid sequence alignment and phylogenetic analysis.

Figure legends

Supplementary Fig. 1 Nucleotide and deduced amino acid sequences of TcLPMO1, LmLPMO1 and OfLPMO1. Predicted secretion signal peptide sequences and the putative LPMO catalytic domains are bolded and boxed, respectively. The conserved cysteine-rich motifs identified at the C-terminus of insect LPMO1 sequences is indicated by gray highlight.

Supplementary Fig. 2 Amino acid sequence alignments of insect LPMO1s. Multiple protein sequence alignment of LPMO1s from several lepidopteran, coleopteran, hymenopteran, dipteran, hemipteran and orthopteran species was made using ClustalW software. Symbols located under the alignment indicate identical (*), highly conserved (:), and conserved residues (.) respectively. Predicted signal peptides and the putative LPMO catalytic domains are underlined and boxed, respectively. The four conserved amino acids (H1, H91, A/S89 and F186/187) involved in the copper binding and the two (Y24 and W168/169) involved in the substrate binding are highlighted in magenta and yellow, respectively. Gray highlight indicates C-terminal

822 stretches consisting of two “6-cysteines-containing internal repeats
823 (C-X_{15}-C-X_3-C-$X_{6\text{-}9}$-C-X_4-C-X_1-C)” where X is any amino acid residue. The
824 6-cysteines in each repeat are indicated by open circles. Amino acid sequences of the
825 catalytic domains of TdAA15A and TdAA15B are also shown above the alignment.
826
827 **Supplementary Fig. 3 Knockdown levels of transcripts of *TcLPMO1* and**
828 ***LmLPMO1* genes by real-time PCR.** (A) cDNAs were prepared from total RNA
829 isolated from three pooled day 1 pupae that had been injected with ds*TcLPMO1* at the
830 last instar larval stage. Transcript level of *TcLPMO1* was presented relative to the level
831 in ds*TcVer*-treated controls. (B) cDNAs were prepared from total RNA isolated from
832 three pooled epidermis of 5th instar day 5 nymphs 2 d after the second ds*LmLPMO1*
833 injection. Expression level of *LmLPMO1* was presented relative to the level in
834 ds*GFP*-treated controls. Data are shown as the mean values ± SE (n = 3).
835
836 **Supplementary Fig. 4 Tissue-specific expression of group II and group III**
837 **LPMOs in *T. castaneum* by RT-PCR.** Transcript abundance of *TcLPMO2* (group II)
838 and seven *TcLPMO* genes belonging to group III in the carcass (CA) and midgut (MG)
839 was determined by real-time PCR. Total RNA was extracted from the tissues of *T.*
840 *castaneum* larvae (n = 10). Expression levels of *TcLPMOs* are presented relative to the
841 levels of expression in carcass (CA).

Supplementary Files

This is a list of supplementary files associated with this preprint. Click to download.

- 09042021SupplimentarymaterialsforTcLPMO1andLmLPMO1.docx